

## Article

# Impact of Metal Accumulation on Photosynthetic Pigments, Carbon Assimilation, and Oxidative Metabolism in Mangroves Affected by the Fundão Dam Tailings Plume

Veronica D'Addazio <sup>1,2,\*</sup>, Monica Maria Pereira Tognella <sup>1,2</sup>, Adriano Alves Fernandes <sup>2</sup>,  
Antelmo Ralph Falqueto <sup>2</sup>, Marcelo Barcellos da Rosa <sup>3</sup>, Ivoney Gontijo <sup>2</sup>  
and Marcelo Antônio de Oliveira <sup>4</sup>

<sup>1</sup> Department of Oceanography Pós-Graduate Program of Environmental Oceanography, Federal University of Espírito Santo, Vitória 29075-710, ES, Brazil; monica.tognella@gmail.com

<sup>2</sup> Department of Agrarian and Biological Sciences, Federal University of Espírito Santo, São Mateus 29932-540, ES, Brazil

<sup>3</sup> Department of Chemistry, Federal University of Santa Maria, Camobi Campus, Santa Maria 97105-900, RS, Brazil

<sup>4</sup> Department of Health Sciences, Federal University of Espírito Santo, São Mateus 29932-540, ES, Brazil

\* Correspondence: veronicadaddazio@yahoo.com

**Abstract:** The effects of iron, manganese, zinc, copper, and lead on the chlorophyll content, carbon assimilation, and the antiradical activity of *Rhizophora mangle* and *Laguncularia racemosa* were evaluated in regions affected by the Fundão dam disruption in Brazil. The mine waste which settled and accumulated in the sediments could represent long-term contamination. It can be expected that the iron oxyhydroxides deposited in the sediments will be solubilized, leading to chronic contamination by trace metals and the accumulation of these metals in the biota. In this sense, biological indicators prove to be important tools to assess this type of damage. The different bioaccumulation of metals by the species revealed that *R. mangle* was more impacted by Mn and Cu and that *L. racemosa* showed alterations in its physiological responses in the presence of Cu, Zn, and Fe. The concentration of these metals in the leaves, with values above previous local reference limits, was associated with reductions in the chlorophyll-a and chlorophyll-b content and carbon assimilation, mainly in *L. racemosa*. The antiradical activity was also altered, suggesting a lower ability of both species to eliminate reactive oxygen species (ROS). A possible reason for the symptoms of oxidative stress may be due to the reduced efficiency of antioxidant defense by Cu<sup>2+</sup> and Zn<sup>2+</sup>. In addition, the presence of Pb in the leaf tissue may be toxic to the fauna and the bioaccumulation of this metal and trace elements can be a way to transfer them into the food web by biomagnification.

**Keywords:** chlorophyll; DPPH<sup>•</sup>; mangrove; *Rhizophora mangle*; *Laguncularia racemosa*; potentially toxic metal; bioaccumulation; bioconcentration factor



**Citation:** D'Addazio, V.; Tognella, M.M.P.; Fernandes, A.A.; Falqueto, A.R.; da Rosa, M.B.; Gontijo, I.; de Oliveira, M.A. Impact of Metal Accumulation on Photosynthetic Pigments, Carbon Assimilation, and Oxidative Metabolism in Mangroves Affected by the Fundão Dam Tailings Plume. *Coasts* **2023**, *3*, 125–144. <https://doi.org/10.3390/coasts3020008>

Academic Editor: Donald C. Barber

Received: 20 December 2022

Revised: 20 March 2023

Accepted: 12 April 2023

Published: 14 April 2023



**Copyright:** © 2023 by the authors. Licensee MDPI, Basel, Switzerland. This article is an open access article distributed under the terms and conditions of the Creative Commons Attribution (CC BY) license (<https://creativecommons.org/licenses/by/4.0/>).

## 1. Introduction

The mangrove ecosystem is one of the main types of natural wetlands along tropical and subtropical coasts and has considerable ecological and commercial value [1,2]. Although mangroves cover only 0.1% of the Earth's continental surface (~81,485 km<sup>2</sup>), they can store large amounts of carbon from the soil because they sequester it faster than most terrestrial ecosystems, in addition to storing more of this chemical element per unit of area compared to terrestrial forests. Therefore, mangrove forests are viewed as one of the most productive and efficient long-term natural carbon sinks [3,4] and are an important ecosystem for storing blue carbon. Despite their importance, Brazilian mangroves have faced serious environmental problems such as the rupture of the Fundão Dam (2015) in Minas Gerais, southeast Brazil. The Fundão rupture is considered the greatest environmental disaster in Brazilian history, with approximately 50 million m<sup>3</sup> of mud spilled. The

intense flow of water and iron ore tailings was transported over 650 km before reaching the Atlantic Ocean (Figure 1), spreading a plume of turbidity over a large area, mainly to the southern coast of Brazil [5–7]. Tailings mud can directly or indirectly affect the Atlantic coastal ecosystems of other states such as Espírito Santo (southeastern Brazil) and Bahia (northeastern Brazil) [8,9]. According to Tognella et al. [10], this environmental disaster is the first opportunity to understand the effect of mining tailings on tropical coastal areas and to identify the damage caused to mangroves.

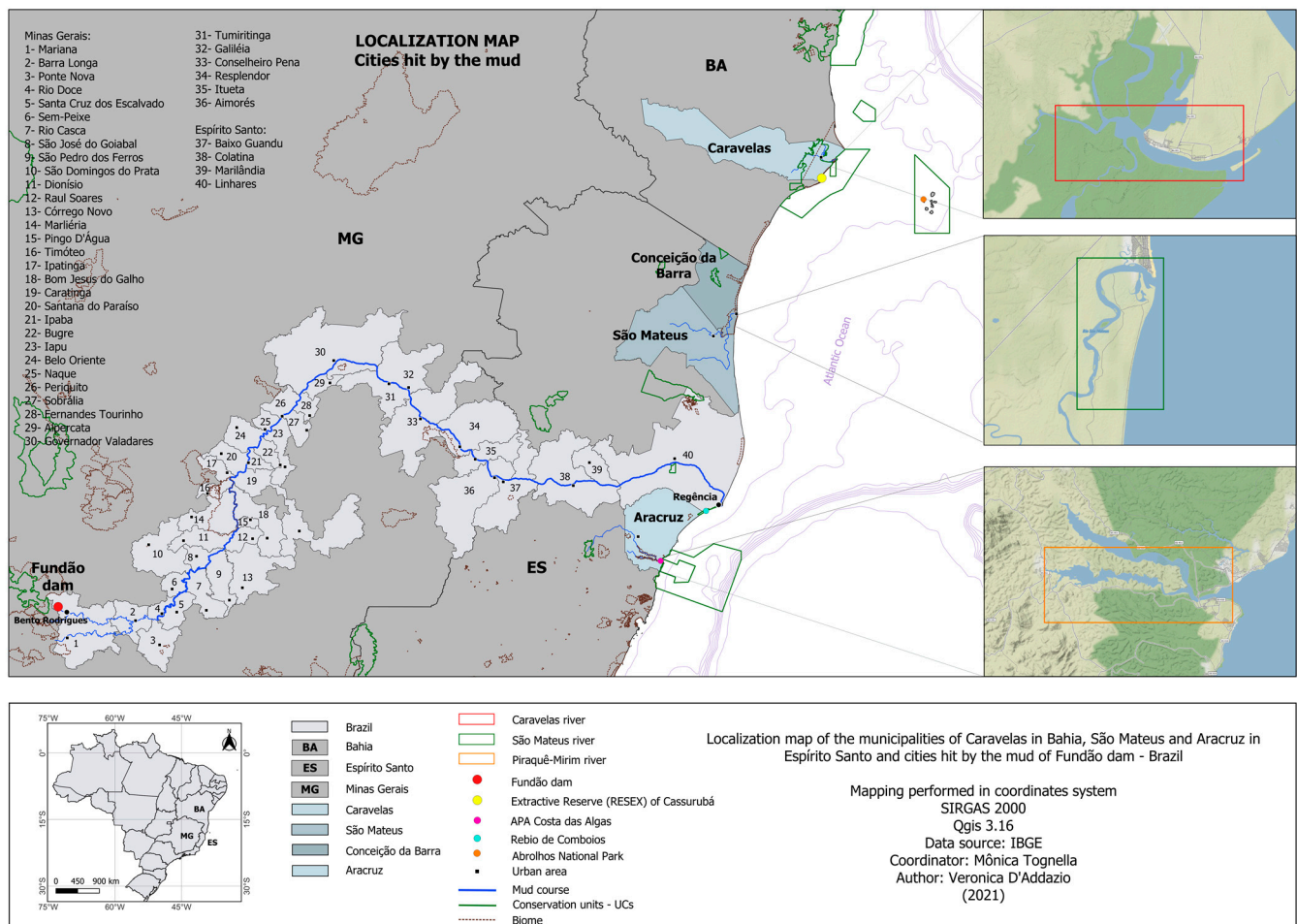


**Figure 1.** Localization of the studied areas: Caravelas River (CR), São Mateus River (SM), and Piraquê-Mirim River (PM) in the states of Bahia and Espírito Santo and the cities affected by the mud from Fundão dam—Brazil.

Naturally, mangroves play an important role in preventing contamination of the estuarine ecosystem. Around the world, some studies that have taken into account the accumulation of metal and nutrients in sediment failed to register toxicity in mangroves [11]. However, metals remain present in the environment for a long time, whether from natural or anthropogenic sources. Thus, they potentially become bioavailable and toxic to the biota at high concentrations [12] due to their potential for bioaccumulation and biomagnification [13], which affects physiological behavior. The highly specific mechanisms and biotic responses of mangrove plants to capture, translocate, and store toxic metals within their physiological ranges are generally selective [14]. However, non-essential elements are also captured by the same transport systems [15]. In this way, essential and non-essential metals are worrying pollutants and represent a threat to mangroves as they are able to cross the entire ecological cycle and can be involved in the ecosystem for a long time [16].

Monitoring the metal levels in these environments provides useful indicators for assessing metal pollution and predicting ecosystem impact [17]. Although some mangrove species demonstrate a relatively high tolerance to trace element pollution [18,19], studies report high concentrations of these elements accumulated in their tissues [20], with a variety of metabolic reactions that cause damage at the cellular level or lead to broader phytotoxic responses [21]. A major consequence is the increased production of reactive oxygen species (ROS) which alter the functional processes of photosynthesis and damage cell membranes, nucleic acids, and photosynthetic pigments [22], especially in the presence of free iron in the cell [23]. The mobility and bioavailability of metals depend not only on their total concentration but also on their association with the solid phase to which they are linked [24]. In addition, soil pH, cation exchange capacity, and salt content also affect these processes [25]. Concomitantly, trace element cycling is a potentially serious problem in mangrove environments [26] since the excessive transfer of heavy metals from sediments to mangrove plants can lead to contamination of the food chain [27].

In this context, the objective of this study was to evaluate the absorption and accumulation of metals as well as their effect on the concentration of photosynthetic pigments, carbon assimilation, and antiradical activity in two mangrove species (*Rhizophora mangle* and *Laguncularia racemosa*) located in three different impacted estuaries that experienced disruption from the Fundão dam in 2015 [28]. After this damage, monitoring should answer some questions about the flora: (1) Will the trace elements from Fundão tailings affect the mangrove ecosystem since they are essential to life? (2) Is there interference of these elements in the physiological performance of the mangrove? (3) Do mangrove species behave similarly to these trace elements?

To answer these questions, the research considers how sediment characteristics influence the concentration of sedimentary metals and trace elements, which in turn determine different patterns of accumulation and translocation in different mangrove species. Our great challenge is the lack of defined baseline levels for the foliar concentration of trace elements and the flora contamination level. Consequently, alterations in the photosynthetic apparatus and the oxidative metabolism of plants must be considered and may be useful tools to monitor the damage caused by metals in the long term, in addition to acting as biological indicators of physiological disorders as these disorders can decrease mangrove productivity on the coast.

## 2. Materials and Methods

### 2.1. Study Area

The areas affected by the ore tailings from the Fundão Dam studied here were the estuaries of Piraquê-Mirim (PM), São Mateus (SM), and Caravelas (CR) (Figure 1). Piraquê-Mirim is an estuary located in Aracruz at 19°55' S, 40°12' W within a protected area on the SE Brazilian coast [29]. This estuary has a Y-shaped morphology and about 12 km<sup>2</sup> of preserved mangroves mostly dominated by *Rhizophora mangle* L. (about 84%), followed by *Laguncularia racemosa* (L.) C.F. Gaertn and *Avicennia schaueriana* Stapf & Leechman ex Moldenke, within tidal flats under a semi-diurnal micro tidal system (<2 m) (Figure 2). The estuary is classified as a tidal domain and presents ebbs (spring tide ebbs = 0.7 ms<sup>-1</sup> versus spring tide floods = 0.54 ms<sup>-1</sup>) with a current velocity greater than the floods [10].

The São Mateus River basin is approximately 103.351 km<sup>2</sup>. It is located at 18°42' S, 39°51' W and it bathes ten cities in the states of Minas Gerais and Espírito Santo, flowing into the Atlantic Ocean from Conceição da Barra city (Figure 2). According to the Instituto Nacional de Pesquisas Espaciais (INPE), in 2013, only 15.425 km<sup>2</sup> (7%) of the entire area of the city was covered by native vegetation. Of these, 1.452 km<sup>2</sup> were mangroves. The dominant plant species were *R. mangle* and *L. racemosa* [30]. The flooded river dominates the ocean during the rainy season, and, in the dry months, the estuary is dominated by waves and tides, which strongly influence the local salinity. In addition, neap tides have a higher ebb flow, i.e., 427.0 m<sup>3</sup>s<sup>-1</sup> [10].

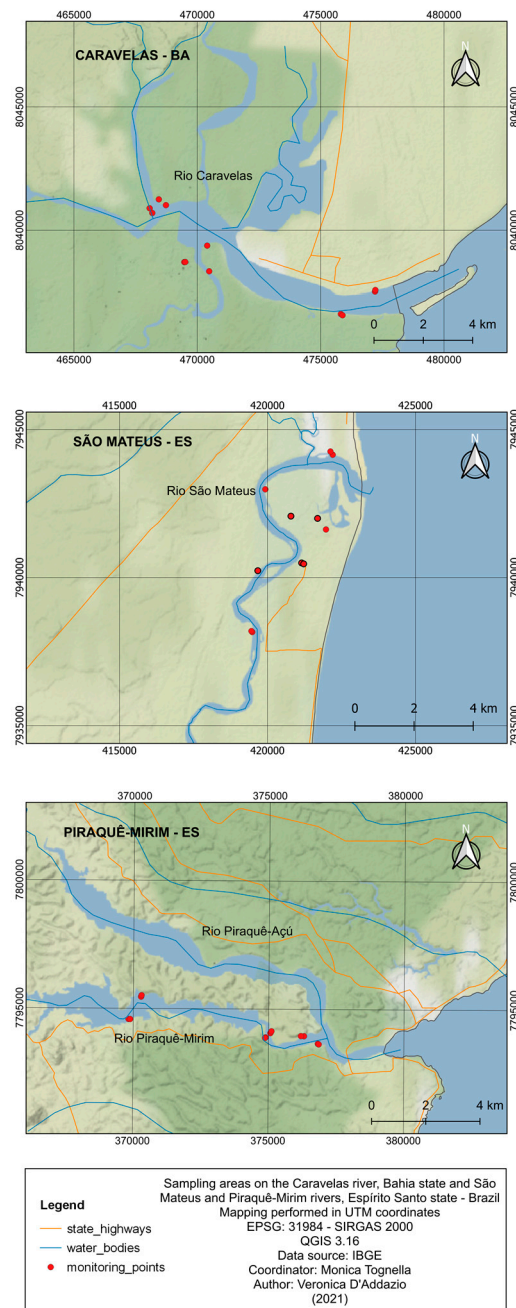


**Figure 2.** Caravelas River in Caravelas city, Bahia; São Mateus River in the São Mateus and Conceição da Barra cities, and Piraquê-Mirim River in Aracruz, Espírito Santo—Brazil.

The Caravelas River estuary ( $17^{\circ}43' S$ ,  $39^{\circ}15' W$ ) is located on the southern coast of the state of Bahia, in the city of the same name. It extends itself towards the continent, where it forms the second most complex mangrove system in northeast Brazil, with an area of  $66 \text{ km}^2$ . This estuary behaves like a typical tidal channel governed by coastal waters, is associated with the Peruípe River mouth, and features an entrance bar approximately 2 km long (Figure 2). The dominant plant species are *R. mangle* and *L. racemosa*. For detailed descriptions of the area and the damage caused by the dam rupture, consult Tognella et al. [10].

The collection and handling of all material followed the current Brazilian legislation with a license from the Ministry of the Environment, under process number 75435/1.

## 2.2. Sediments

Sediment samples were collected in the intertidal zones within the mangroves using 50 cm collectors built with a polyvinyl chloride (PVC) tube. Twenty-four sediment samples were collected at points previously described [10] in the Piraquê-Mirim, São Mateus, and Caravelas Rivers at a depth of 0–5 cm. After collection, the samples were placed in previously identified plastic bags and stored at  $-10\text{ }^{\circ}\text{C}$ .

## 2.3. Granulometry, Organic Matter, and Calcium Carbonate

The granulometry analysis determined the fractions of sand, silt, and clay in the sediment samples. Approximately 50 g of the crude sample was washed with water to remove the salts; then, the analyses were performed according to Dias [31]. First, the sample was washed with water to remove the salts, using the decantation technique, three times. Subsequently, the coarse (sand + gravel) and fine (silt + clay) fractions were separated. The beaker containing the fine fraction was left to rest until the complete deposition of the suspended sediment occurred. After decanting, the excess water was carefully drained with a hose and the total removal of organic matter in the sample was conducted by burning it with hydrogen peroxide ( $\text{H}_2\text{O}_2$ ) at 30%. After the firing, the sample was washed three times in the beaker itself. In these samples, the mud fraction was analyzed using a laser granulometer, Mastersizer 2000 from Malvern Instruments, according to the methodology adapted from Dias [31]. The beaker containing the coarse fraction (after the water was drained) was placed in an oven at  $40\text{ }^{\circ}\text{C}$  to dry the sample. After drying, the sediment was weighed and proceeded to dry fractionation. The sand fraction was passed through dry sieving, which consists of using a set of sieves with mesh screens from 2 mm to 0.063 mm placed in a mechanical shaker for 15 min. After sieving, each portion of the sediment, according to its granulometry, was weighed and spread out. The grain size scale used was that of Wentworth [32], in which fractions greater than 0.063 mm are classified as sand/gravel and the smallest as silt/clay [33].

The content of total organic matter (OM) present in the sediments was measured using the calcination method, which consists of burning the OM at high temperatures. The samples were subjected to a temperature of  $450\text{ }^{\circ}\text{C}$  in a muffle for 4 h. The OM mass is defined by the weight of the sediment before burning minus the weight after burning, according to the modified Walkley–Black method [34].

For the determination of calcium carbonate ( $\text{CaCO}_3$ ), about 20 g of the lyophilized crude sample was weighed and dried. The dry sample was placed in a fume hood for the slow and gradual addition of HCl (30%). The procedure continues until the addition of HCl causes no further reaction (bubbling). After the carbonate burning, the sediment was washed three times with water and dried in an oven at  $40\text{ }^{\circ}\text{C}$ . After drying, the sample was weighed again and the calcium carbonate content was considered as the pre-burn sediment subtracted from the post-burn sediment, corrected for percentage.

## 2.4. Metals in Sediments

The analysis of metals in the sediments was performed according to the USEPA 3051A method [35]. The elements analyzed by ICP-MS (inductively coupled plasma mass spectrometry; Agilent, CX7500) were Cu, Fe, Mn, Pb, and Zn ( $\text{mg kg}^{-1}$ ). The mean value of the depths 0–5 cm was used in this study. The TEL (thresholds effects|Levels)—NOAA was considered the reference point of contamination when possible [36]. For Fe and Mn, the apparent effect limit (AET) value was used.

## 2.5. Salinity

The salinity measurements of the interstitial water were performed concomitantly with the leaf collections. The salinity of the interstitial water was obtained after percolating the water into the polyvinyl chloride (PVC) tube, previously installed, using a Hach multiparameter sensor calibrated with a standard solution before each sampling.

## 2.6. Leaf Samples

Twenty fully expanded mature leaves were collected from five individuals of the species *R. mangle* (Rh) and *L. racemosa* (Lg), according to their existence in the plots in the PM, SM, and CR estuaries. After collection, the leaves were packed in paper bags and identified according to each sampling station, for further analysis of leaf metals and antiradical activity. The same number of leaves was collected for the analysis of photosynthetic pigments. These samples were stored on ice before arriving at the Mangrove Ecology Laboratory, where they were frozen at  $-30\text{ }^{\circ}\text{C}$  until the analysis.

## 2.7. Leaf Analysis of Macro and Micronutrients

For the determination of macro and micronutrients and antiradical activity, the leaves were dried at  $65\text{ }^{\circ}\text{C}$  in a forced circulation oven until constant weight. Then, the samples were ground in a Wiley mill (Tecnal brand; model TE-650/1) with 20 mesh sieves. For leaf analysis, the following nutrients were considered: iron (Fe), manganese (Mn), zinc (Zn), copper (Cu), and lead (Pb), all in  $\text{mg kg}^{-1}$ .

Fe, Mn, Zn, and Cu were analyzed by atomic absorption spectrophotometry [37] and Pb was analyzed according to Malavolta et al. [38]. Past data from Cuzzuol and Campos [39], Machado et al. [40], and Souza et al. [41] were our referential baseline. The Fe and Mn were evaluated due to their contribution to the dam sediments; the other elements are toxic to the biota and associated with Fe and Mn oxyhydroxides. The analyses were carried out by a certified company, with reference to the Quality Management System, corresponding to the ISO 9001:2015 Standard with Environmental License and Registration with the Ministry of Agriculture (MAPA).

## 2.8. Carbon Assimilation

To measure  $\text{CO}_2$  assimilation ( $A-\mu\text{mol m}^{-2}\text{s}^{-1}$ ) portable photosynthesis meters (Infrared gas analyzer, IRGA), models LCi, LCi T, and Lcpro T (ADC, Bio Scientific Ltd. Hoddesdon, UK), were used. The number of samples was the same as in the other foliar analyses.

## 2.9. DPPH• (2,2-Diphenyl-1-picrylhydrazyl)

Tests with DPPH• were performed to assess antioxidant activity, with all solutions of the dry extracts diluted in methanol. Solutions that had already been diluted were referred to as working solutions (WS). The tests were performed by adding 15  $\mu\text{L}$ , 25  $\mu\text{L}$ , and 35  $\mu\text{L}$  aliquots of each WS in cuvettes containing 3.0 mL of DPPH• in a  $0.2\text{ mmol L}^{-1}$  methanol solution, and keeping the reaction in the dark for 60 min before spectrophotometric measurements. These were performed on a Lambda 16 spectrophotometer, from the Perkin Elmer brand, by monitoring the absorbance of the samples at 517 nm. The blank consisted of 3.0 mL of methanol containing 15  $\mu\text{L}$ , 25  $\mu\text{L}$ , or 35  $\mu\text{L}$  of the respective WS. The negative control was a solution containing only DPPH•  $0.2\text{ mmol L}^{-1}$  in methanol. The calculation of the DPPH• scavenges percentage was performed according to Dal Prá et al. [42] and represented as IC50 values (concentration necessary to inhibit 50% of the DPPH• radical).

## 2.10. Photosynthetic Pigments

The samples frozen at  $-30\text{ }^{\circ}\text{C}$  (fresh mass) were processed in liquid nitrogen ( $\text{N}_2$ ) and transferred to test tubes containing 15 mL of a 90% acetone solution +  $0.5\text{ g L}^{-1}$  of calcium carbonate ( $\text{CaCO}_3$ ). After this process, the test tubes were stored at a temperature of  $2\text{ }^{\circ}\text{C}$  for 48 h for complete pigment extraction [43]. Thereafter, the samples were filtered and the supernatant was stored in amber flasks at  $-30\text{ }^{\circ}\text{C}$  until analysis.

An aliquot of the supernatant was clarified in a  $0.45\text{ }\mu\text{m}$  syringe filter and injected into a reverse phase column. The pigment separation was performed by high-pressure liquid chromatography (HPLC) on Waters “e2695 Alliance” equipment, Waters photographic diode spectrophotometric detector “2998 Photodiode Array Detector” (PDA 2998), Waters columns “XBridge C18” ( $3.5\text{ }\mu\text{m}$ ,  $4.6\text{ mm} \times 50\text{ mm}$ ), and “Symmetry C18” ( $3.5\text{ }\mu\text{m}$ ,

3.9 mm × 5 mm). The chromatographic data analysis system used was the Waters Empower 3 software. The mobile phase was composed of a linear gradient of methanol (eluent A), 0.5 M ammonium acetate (eluent B), and acetone (eluent C) with the following gradient: 0 min (80:20:0 v/v/v), 2 min (80:20:0), 15 min (80:0:20), 17.5 min (80:0:20), 22 min (0:0:100), 25 min (80:20:0), and 30 min (80:20:0). The flow of the mobile phase was constant at 1 mL min<sup>-1</sup> and the column temperature was adjusted to 25 °C. The injection volume was 50 µL. The chlorophyll absorption spectrum was adjusted between 380 and 750 nm, with a wavelength of 440 nm. Isolated pigments were identified by comparing their absorbance spectra and retention times with those of chlorophyll-a (Sigma C5753) and chlorophyll-b (Sigma C5878). The peak areas found in the extracts were interpolated in the standard curves to quantify the concentration of pigments in the analyzed samples. The values are presented in µg g<sup>-1</sup>.

#### 2.11. Bioconcentration Factor

The bioconcentration factor (BCF) was assessed according to MacFarlane et al. [18] and is defined as the ratio of the metal concentration between the leaf tissue and the sediment.

$$\text{BCF} = \frac{\text{Metal concentration in Plant}}{\text{Metal concentration in Sediment}}$$

#### 2.12. Statistical Analysis

The analyzed data addressed the three estuaries and the species *R. mangle* and *L. racemosa*. All data were subjected to an analysis of variance (ANOVA) and Tukey's test, when necessary, at a level of 5% probability using the Genes 3.1 software [44]. The Principal Component Analysis (PCA) was performed with the aid of the R Core Team software [45], using the packages "ggplots" [46], "FactoMineR" [47], "Factoextra" [48], and "FactoInvestigate" [49]. The results correspond to samples collected from February 2019 to February 2020. Leaf collections were performed every two months and sediment collections every six months.

### 3. Results

The granulometric characteristics and metal concentrations of the sediments were different, depending on the predominant species in the sampling sites and the oceanographic conditions such as tides, waves, and salinity distribution in the estuaries. Higher values of clay, silt, CaCO<sub>3</sub>, manganese (Mn-s), zinc (Zn-s), and lead (Pb-s) were found in Caravelas for sediments dominated by *R. mangle* and *L. racemosa* (Figure 3A,B,E,H,I,K) where there was also a lower concentration of sand (Figure 3C). Concerning organic matter (OM), there was a higher percentage in the sediments from the Piraquê-Mirim and Caravelas estuaries with a predominance of *R. mangle* and the sediments of the São Mateus and Caravelas estuaries with *L. racemosa* (Figure 3D). The salinity variable showed similar behavior in sediments dominated by both species (Figure 3F). The iron content (Fe-s) was higher in sediments of *R. mangle* in Piraquê-Mirim and Caravelas (Figure 3G), although sediments of *L. racemosa* showed high values of the metal in Caravelas. The copper (Cu-s) concentration was similar between the sediments of both species located in the Piraquê-Mirim estuary, with higher values compared to the other two estuaries (Figure 3J).

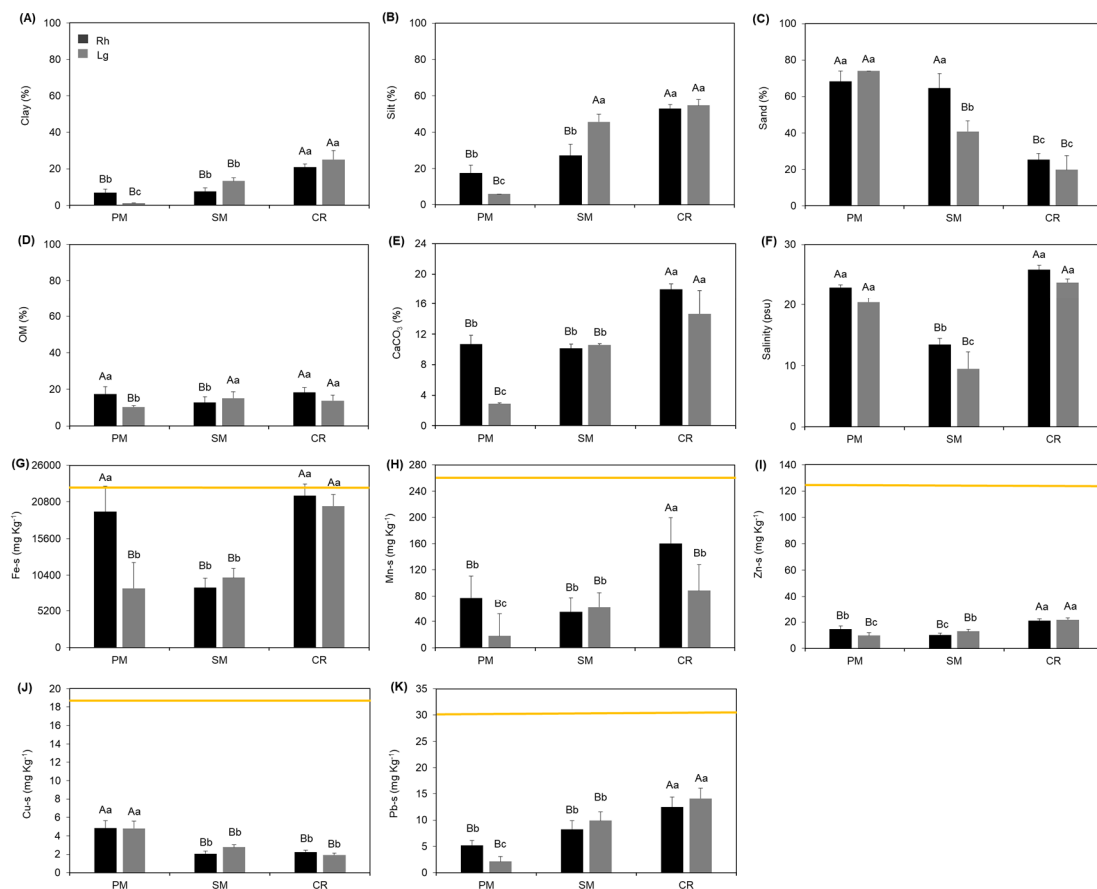


**Figure 3.** Percentage of clay (A), silt (B), sand (C), organic matter (OM) (D) and CaCO<sub>3</sub> (E), salinity (F), and concentration of metals iron (Fe-s) (G), manganese (Mn-s) (H), zinc (Zn-s) (I), copper (Cu-s) (J), and lead (Pb-s) (K) in sediments predominated by *Rhizophora mangle* (Rh) and *Laguncularia racemosa* (Lg) species, located in the Piraquê-Mirim (PM), São Mateus (SM) and Caravelas (CR) estuaries. Values are expressed as the mean  $\pm$  SD. Means followed by the same letter do not differ statistically by Tukey's test ( $p < 0.05$ ). Capital letters represent the species and lowercase letters represent estuaries. Yellow lines represent the values used as a reference for sediments: National Oceanic and Atmospheric Administration—NOAA reference limits (TEL and AET) [36].

In the comparative analysis between the mangrove species, a significant difference was observed between *R. mangle* and *L. racemosa* when compared to each other and the behavior of each species in the evaluated estuaries. Figure 4A,B show the photopigment data, with a significant difference between the estuaries. There was a higher concentration of chlorophyll-a (Chla) and chlorophyll-b (Chlb) for both species located in the Piraquê-Mirim estuary. The *R. mangle* located in Caravelas also showed higher values of Chla (Figure 4A) while a lower ratio between chlorophyll-a and chlorophyll-b (Chla/Chlb) and lower values of Mg-f were observed in *L. racemosa* (Figure 4C,K). Carbon assimilation (A) was lower in both species located in the São Mateus and Caravelas estuaries (Figure 4D). The lowest scavenging activity against the DPPH• radical (high IC50) was observed in *R. mangle* in the São Mateus estuary, while for *L. racemosa*, high IC50 values were found in São Mateus and Caravelas (Figure 4E). Regarding metal concentrations in the leaves, *L. racemosa* had a higher concentration of iron (Fe-f) compared to *R. mangle*, mainly when analyzed in the São Mateus River (Figure 4F). The Fe-f values found for *R. mangle* were similar between the estuaries, with no statistically significant difference. A different behavior was observed for the metal manganese (Mn-f) which presented higher values for the species *R. mangle*. Comparing the estuaries, there was a lower concentration of Mn-f in Piraquê-Mirim for *R. mangle* and Piraquê-Mirim and Caravelas for *L. racemosa* (Figure 4G). There was a significant difference

between species concerning leaf zinc (Zn-f). The highest concentrations occurred for *L. racemosa* in all estuaries, except in Piraquê-Mirim. For *R. mangle*, there was no significant difference in zinc concentration between estuaries (Figure 4H). A higher concentration of copper (Cu-f) was observed for *L. racemosa* in São Mateus and Caravelas. Similar results were observed in *R. mangle* (Figure 4I). The species *R. mangle* had the highest lead value (Pb-f) in the São Mateus estuary; the metal concentration did not vary between estuaries for *L. racemosa* (Figure 4J).

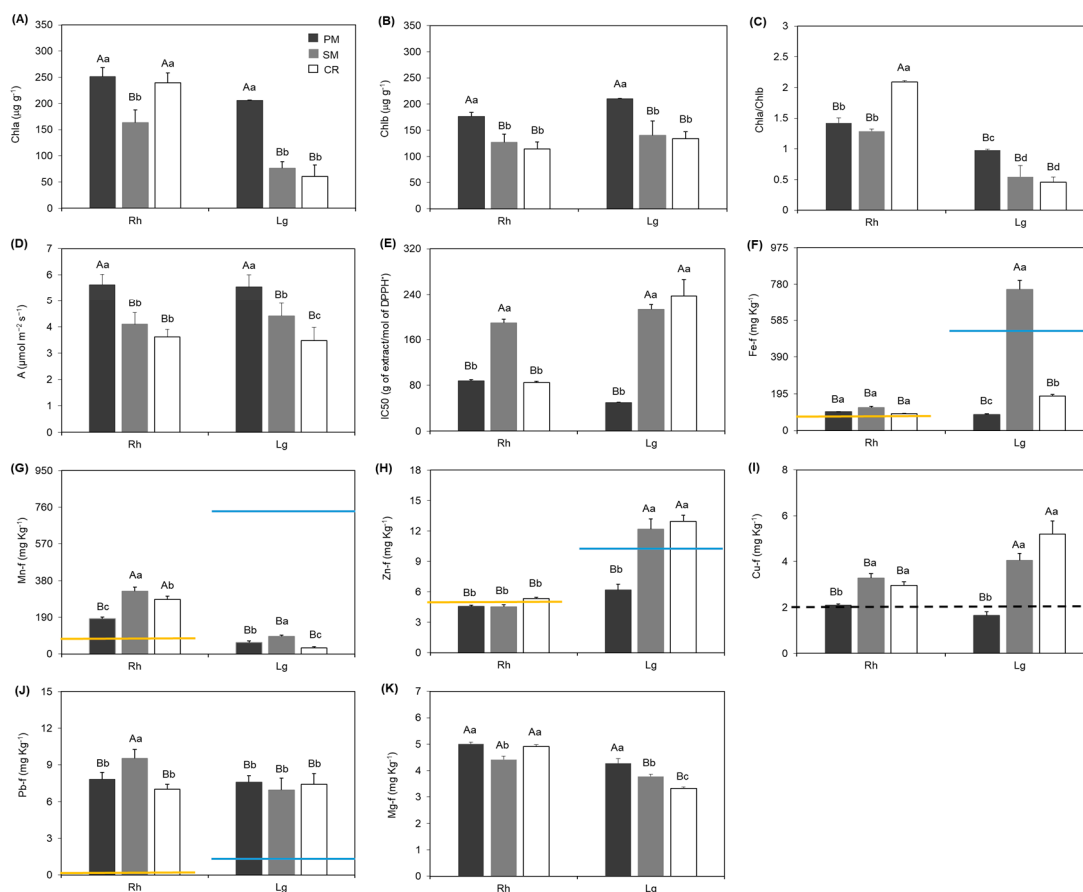


**Figure 4.** The concentration of chlorophyll-a (Chla) (A), chlorophyll-b (Chlb) (B), chlorophyll-a/chlorophyll-b ratio (Chla/Chlb) (C), carbon assimilation (A,D), antiradical activity against DPPH<sup>•</sup> (IC50) (E), and the leaf metals iron (Fe-f) (F), manganese (Mn-f) (G), zinc (Zn-f) (H), copper (Cu-f) (I), lead (Pb-f) (J), and magnesium (Mg-f) (K) in *Rhizophora mangle* (Rh) and *Laguncularia racemosa* (Lg) species, located in the Piraquê-Mirim (PM), São Mateus (SM), and Caravelas (CR) estuaries. Values are expressed as the mean  $\pm$  SD. Means followed by the same letter do not differ statistically by Tukey's test ( $p < 0.05$ ). Capital letters represent the species and lowercase letters represent estuaries. Yellow lines represent the values used as a reference for the species *R. mangle*; blue lines represent values used as a reference for *L. racemosa*; and a dashed black line represents the value used as a reference for both species. References: [39–41].

All data from Figures 3 and 4 represent the mean values of the metals analyzed in the sediments and the leaves. However, considering the raw values of each metal in the respective estuaries and mangrove species, it was observed that a percentage of the sediment samples presented values above the NOAA AET limits [36]. This also occurred for leaf samples, with raw data above the values used as a reference, as reported by Cuzzuol and Campos [39], Souza et al. [40], and Machado et al. [41]. A summary is presented in Table 1.

**Table 1.** Percentage of samples of sediments and leaves of *Rhizophora mangle* (Rh) and *Laguncularia racemosa* (Lg) collected in the Piraquê-Mirim, São Mateus, and Caravelas rivers with values above the reference. Reference values for sediments: National Oceanic and Atmospheric Administration—NOAA reference limits (TEL and AET) [36]. Reference values for mangrove species: [39–41]. Fe: iron; Mn: manganese; Zn: zinc; Cu: copper; Pb: lead; PM: Piraquê-Mirim; SM: São Mateus; and CR: Caravelas.

	Percentage (%)								
	Sediment <sup>1</sup>			Leaf <sup>2</sup>					
	PM	SM	CR	PM		SM		CR	
			Rh	Lg	Rh	Lg	Rh	Lg	
Fe	36	7	46	76	0	93	60	78	0
Mn	9	0	21	0	20	0	53	0	0
Zn	0	0	0	37	0	23	60	58	50
Cu	2	0	0	52	20	70	100	56	40
Pb	0	5	14	100	100	100	100	100	100

<sup>1</sup> Sediment reference values (mg kg<sup>-1</sup>)—Fe: 22,000; Mn: 260; Zn: 124; Cu: 18.7; and Pb: 30.24. <sup>2</sup> Leaf reference values for Rh (mg kg<sup>-1</sup>)—Fe: 72–92.6; Mn: 738.4–929.6; Zn: 5.0; Cu: 2.0; and Pb: 0.02–0.11. <sup>2</sup> Leaf reference values for Lg (mg kg<sup>-1</sup>)—Fe: 523.3–655.1; Mn: 79.9–112.4; Zn: 10.2–15.2; Cu: 2.0; and Pb: 1.3–8.9.

In general, the results of the principal components analysis (PCA) explained 100% of the joint variability of the data in the first two axes for both species (Figure 5). In *R. mangle*, the variables Zn-s, Pb-f, Fe-f, Fe-s, salinity, Mn-s, OM, Zn-f, DPPH<sup>•</sup>, Chla, clay, and sand presented the highest contribution, in order of importance, and accounted for 59.18% of the variability in dimension 1 (PCA1). On the other hand, although with less significance (40.82%), dimension 2 (PCA2) showed the association of Chlb, Cu-s, Cu-f, Mn-f, A, Pb-s, and silt (Figure 5A). Pearson’s linear correlation for *R. mangle* can be seen in Figure 5B.

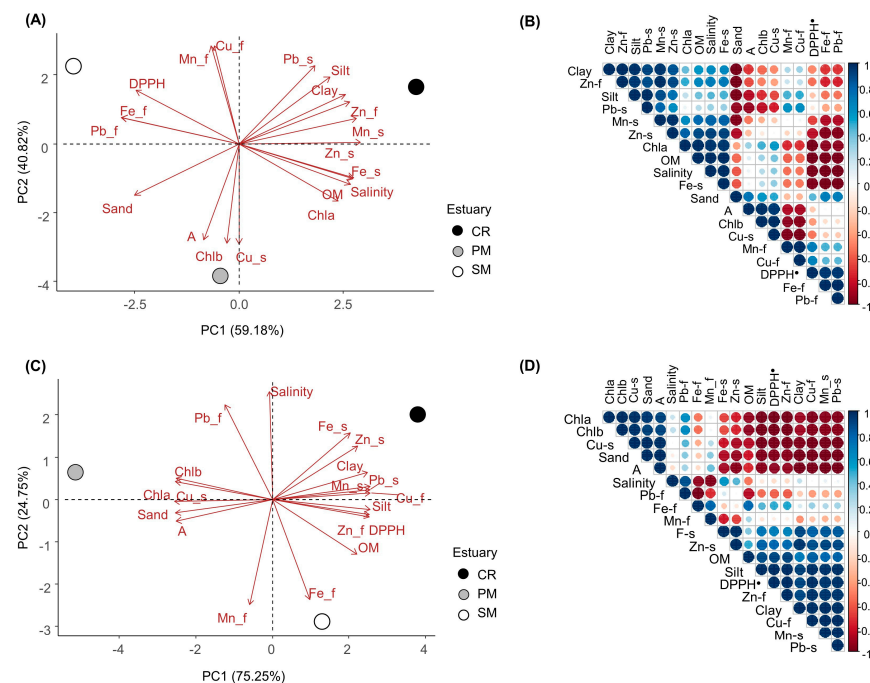


**Figure 5.** Principal components analysis plot (PCA) and Pearson’s linear correlation of *Rhizophora mangle* (A,B) and *Laguncularia racemosa* (C,D) species in the Piraquê-Mirim (PM), São Mateus (SM), and Caravelas (CR) estuaries. Metals in sediment: iron (Fe-s), manganese (Mn-s), zinc (Zn-s), copper (Cu-s), and lead (Pb-s); metals in leaf tissue: iron (Fe-f), manganese (Mn-f), zinc (Zn-f), copper (Cu-f), and lead (Pb-f); OM: organic matter; Chla: chlorophyll-a; Chlb: chlorophyll-b; A: carbon assimilation; and DPPH<sup>•</sup>: 2,2-Diphenyl-1-picrylhydrazyl.

In the PCA of *L. racemosa* (Figure 5C), Zn-s, Mn-s, Fe-f, Pb-f, Fe-s, salinity, OM, Zn-f, clay, sand, Chla, and DPPH<sup>•</sup>, accounted for 75.25% of the variability in dimension 1 (PCA1), while Cu-s, Chlb, Cu-f, Mn-f, A, Pb-s, and silt and were associated with dimension 2 (PCA2) with 24.75% variability. Figure 5D shows Pearson's linear correlation for this specie.

The bioconcentration factor for both species can be seen in Table 2. BCF values between 0.01 and 0.1 represent a low metal bioconcentration in the leaf; between 0.1 and 1.0 correspond to medium bioconcentration; and 1.0 and above indicate high bioconcentration.

**Table 2.** Bioconcentration factors (BCF = metal concentration in leaf tissue/metal concentration in sediments) of *Rhizophora mangle* (Rh) and *Laguncularia racemosa* (Lg) species in the Piraquê-Mirim, São Mateus, and Caravelas estuaries. Fe: iron; Mn: manganese; Zn: zinc; Cu: copper; and Pb: lead.

	BCF				
	Fe	Mn	Zn	Cu	Pb
<i>Rhizophora mangle</i>					
Piraquê-Mirim	0.01	2.36	0.32	0.43	1.50
São Mateus	0.01	5.97	0.46	1.37	1.15
Caravelas	0.04	1.76	0.25	1.27	0.56
<i>Laguncularia racemosa</i>					
Piraquê-Mirim	0.01	3.31	0.64	0.34	3.56
São Mateus	0.08	1.47	0.94	1.47	0.70
Caravelas	0.01	0.36	0.61	3.21	0.53

#### 4. Discussion

Granulometry and OM content are important factors that affect the distribution of trace metals [50] and their retention time in sediment [51]. Fine-grained sediments tend to have relatively higher metal contents, partly due to the high specific surface of the particles which increases the surface adsorption of the mineral to OM and the activity of microorganisms that alter the microenvironment, causing a lower oxidation state [52]. In this study, the clay and silt fractions contributed to higher levels of the metals Fe-s, Mn-s, Zn-s, and Pb-s for both species located in the Caravelas River. In this estuary, the contribution of finer sediments was more outstanding than Piraquê-Mirim and São Mateus (Figure 3). The predominance of finer sediment in the Caravelas estuary is due to the influence of the tides on river flows. The extensive tidal plain in this estuary functions as a sink for particulate matter in suspension, except in the dry season. The adsorption capacity of OM can be observed in the *R. mangle* forest sediment, with a positive correlation between OM and the trace elements Fe-s ( $r = 0.99$ ,  $p < 0.05$ ), Mn-s ( $r = 0.78$ ,  $p < 0.05$ ), and Zn-s ( $r = 0.90$ ,  $p < 0.05$ ). The Piraquê-Mirim estuary recorded the lowest values of Fe-s, Mn-s, Zn-s, and Pb-s in the sediment, occurring in the *L. racemosa* forest. This seems to be slightly related to it having the lowest amount of OM but mostly to the absence of clay in this area [53]. These results confirm the interaction of clay with the elements in question. This granulometric fraction is responsible for the sorption/desorption mechanisms induced by the trace element loads. In addition to the question of sediment granulometry and its association with metals, Fe facilitates the precipitation of toxic metals in mangrove sediments [54]. This ability can increase contamination and result in long-term toxicity.

Significant and positive correlations of Fe were formed with the trace elements Mn ( $r = 0.82$ ,  $p < 0.01$ ) and Zn ( $r = 0.93$ ,  $p < 0.01$ ) for the sediments of *R. mangle*. The same occurs between Fe and the elements Mn ( $r = 0.85$ ,  $p < 0.01$ ), Zn ( $r = 0.98$ ,  $p < 0.01$ ), and Pb ( $r = 0.84$ ,  $p < 0.01$ ) for the sediments of *L. racemosa*. This interaction suggests adsorption in the form of Fe oxides/hydroxides, which is associated with the transport and availability of metals that influence exchanges at the water-sediment interface [11,55,56]. This behavior can be observed in the sediments of both species and is justified by the higher concentrations of Fe-s, mainly in Caravelas, which corresponds to the highest concentrations of the other elements, except for Cu-s. According to Kabata-Pendias [57], the high sorption capacity

of Fe oxides (and also Mn) allows for the accumulation of metals mainly in nodules and Fe-rich points. This same author reported that the pH and redox status (Eh) govern all oxidation-reduction reactions in the soil. The reduction of  $\text{Fe}^{3+}$  and  $\text{Mn}^{4+}$  (i.e., insoluble oxyhydroxides) to  $\text{Fe}^{2+}$  and  $\text{Mn}^{2+}$ , for example, has an important effect on the bioavailability of the metal [58,59]. Fe oxyhydroxides deposited in sediments can be expected to be solubilized (by microorganisms and organic ligands), leading to chronic contamination by trace metals and the accumulation of these metals in the biota. In this context, the chronic impact of tailing deposition in estuaries is likely to last longer than expected, especially considering that the Fe redox cycle can trigger different biogeochemical processes [9]. The three estuaries have a semidiurnal tide and the *L. racemosa* forest in Piraquê-Mirim is less flooded. These environmental conditions can explain the different results registered by the metal concentrations between the habitat species, in addition to the granulometry of the sediment.

Still, regarding Fe and Mn, the previous maximum values (based on past studies developed in the Piraquê-Açú and Mirim region) were close to the minimum observed for all collection stations in the period considered in this study, which corroborates the confirmation of an allochthonous source to the estuary resulting from the Fundão Dam failure [60,61].

The Cu content is closely associated with soil texture and generally has lower levels in sandy soils and higher levels in clayey soils [57]. Differently, it was observed in this study that higher Cu values in the sediment were associated with the sandy fraction (Figure 5). Furthermore, the lower OM content and higher sand content suggest that lower concentrations of the metal are linked to the sediment and, therefore, more available for plant uptake. However, such characteristics do not necessarily indicate bioavailability [62], and this behavior is corroborated by the lower concentration of Cu-f and BCF recorded for both species in the Piraquê-Mirim estuary (Figure 4, Table 2). On the other hand, bioaccumulation was observed in São Mateus and Caravelas, places that presented lower concentrations of Cu-s (Figure 3), but with higher Cu-f results than in Piraquê-Mirim, suggesting that in these environments Cu did not occur in residual form, but is bioavailable to plants. For *L. racemosa*, the increase in Cu-f was associated with a high concentration of Mn-s ( $r = 0.99$ ,  $p < 0.05$ ), suggesting the association of Cu with Mn (and also Fe in some cases) oxyhydroxide phases and its bioavailability [62]. The bioavailability of Cu to plants is possible by a disjunctive pathway. In this mechanism, the dissociated metal ion comes into pores with water and is taken up further by the roots [63].

According to Kabata-Pendias [57], the distribution of Pb in soils shows a positive correlation with the fine particle size fraction. Pb is mainly associated with sediments with a higher content of clay, silt, Fe, and Mn, in addition to  $\text{CaCO}_3$  (Figure 3). Considered as one of the main metal binding phases present in sediments,  $\text{CaCO}_3$  is classified as a geochemical support in the retention of metallic elements, which explains the interaction with certain metals [64]. The three domain sites for *L. racemosa* showed all these characteristics, with positive correlations between Pb and silt ( $r = 0.98$ ,  $p < 0.05$ ), clay ( $r = 0.98$ ,  $p < 0.05$ ), Fe ( $r = 0.84$ ,  $p < 0.05$ ), Mn ( $r = 0.99$ ,  $p < 0.05$ ), and  $\text{CaCO}_3$  ( $r = 0.91$ ,  $p < 0.05$ ). For sediments in the presence of *R. mangle*, there was only a correlation between Pb and silt ( $r = 0.98$ ,  $p < 0.05$ ) (Figures 3 and 5). Sipos et al. [65] reported that Pb mobilization is generally slow but, in some soils, the formation of the Pb-organic matter complex can increase its solubility.

Queiroz et al. [9] emphasized that the concentration of metals found mainly in the surface layers of sediments indicates trace metal enrichment caused by tailings. Although the average values of the metals were below the limits reported by the NOAA [36], there were samples with excessive concentrations of metals, mainly iron (Table 1). Considering the environmental conditions that affect the estuarine soil, the limit values may not represent the real environmental risk. Their association with  $\text{CaCO}_3$  indicates an ocean source. The estuaries are under the influence of the flood of the Doce River, and the transport of the sediments and trace elements to the north or south of its mouth is related to littoral drift, prevailing seasonal winds, and coastal currents [10].

In general, mangroves are considered permanent sinks for Zn, Cu, and Pb [54,56]. However, as can be seen in the results referring to leaf metals, there is a transfer and accumulation of these elements to the leaves. In this way, the monitored areas that showed high concentrations of some metals in the different plots in all estuaries indicate potential contamination in the biota [61]. The study areas are an important source of marine resources for the traditional community. The Municipal Sustainable Development Reserve (RDS) Piraquê-Açu and Piraquê-Mirim produce resources for indigenous villages and artisanal fishermen, shellfish gatherers, and crab collectors residing in their surroundings [66]; the Extractive Reserve (RESEX) of Cassurubá, located in Caravelas and nearby municipalities, is part of the Central Ecological Corridor of the Atlantic Forest, which encompasses the entire state of Espírito Santo and part of Bahia, and is important in the exploitation of natural resources and their conservation [67].

According to Lutts and Lefèvre [68], the translocation of metals in plants is positively influenced by salinity and, consequently, greater absorption occurs. In this study, the highest values of Fe, Mn, Cu, and Pb found in the leaf tissue of *R. mangle* occurred in the estuary of São Mateus, the area with lower salinity (Table S1). These data are corroborated by the negative correlations between the salinity variable and Fe-f ( $r = -0.99, p < 0.01$ ), Mn-f ( $r = -0.55, p < 0.01$ ), Cu-f ( $r = -0.53, p < 0.01$ ), and Pb-f ( $r = -0.99, p < 0.01$ ). For *L. racemosa*, a negative correlation only occurred between salinity and Fe-f ( $r = 0.93, p < 0.01$ ) and Mn-f ( $r = 0.96, p < 0.01$ ) (Figures 3 and 4). Such behavior can be attributed to the geochemical heterogeneity of the sediment, the influence of the physiological and anatomical characteristics of the species involved in the metal exclusion mechanisms [69], and the bioavailability of the metal. Lacerda et al. [70] and Medina et al. [71] observed that the concentrations of metals in mangrove leaves do not correlate with the nutrient content of the sediment, revealing the differential absorption of ions by plants. Arrivabene et al. [72] considered that a greater foliar absorption of Fe may occur due to pH conditions since values between 5.5 and 7.0 are more favorable for the absorption of nutrients; this is what may have happened with *L. racemosa* in the São River Mateus (Figure 4C) where the pH varies from slightly acidic to neutral [73]. Otherwise, Mn does not form stable sulfides and some species such as *R. mangle* may have a higher concentration of this metal in the leaf tissue as a result of the solubilization of Mn in the reducing conditions typical of the mangrove ecosystem, making this metal more bioavailable than others [74]. Such behaviors explain why the *R. mangle* and *L. racemosa* plants absorb metals in different concentrations.

The preferential incorporation of Mn by *R. mangle* and Fe by *L. racemosa* agrees with the results described by other authors [39,73]. According to Lacerda et al. [75], the salt input control mechanism can also affect the absorption of metals by plants. Thus, the mechanism of exclusion of salt present in *R. mangle* could prevent the entry of trace elements such as Fe, Zn, Cu, and Pb, causing a decreased concentration of these elements in the leaf tissue. Despite this characteristic, most of the metals analyzed in the leaves of *R. mangle* presented values above those used as references in this study. The same can be observed for *L. racemosa* (Figure 4, Table 1).

Although iron plates interfere with the absorption of some metals considered toxic to plants, the presence of Zn and Cu in the leaf tissues demonstrates that the absorption process is not controlled only by the presence of these plates. The bioavailability of Cu and other elements in mangrove sediments depends on their chemical speciation [62]. The higher concentration of Zn and Cu in the leaf tissue of *L. racemosa*, compared to *R. mangle*, confirms the interspecific difference in the absorption and the capacity for the accumulation of metals between the two species. This differential behavior between mangrove species is corroborated by other studies around the world. Copper was the trace element that most accumulated in the tissues (roots, stems, and leaves) of *Lumnitzera racemosa* [56]. This species belongs to the Combretaceae Family, like *L. racemosa*, and occupies a niche in the Indo/Pacific region similar to *L. racemosa* in South America. The positive correlation between Zn and Cu in *L. racemosa* ( $r = 0.97, p < 0.05$ ) (Figure 5) can be attributed to the active absorption process of these elements in the soil, in which there is competition for the same

carrier site between them [76]. Queiroz et al. [9] reported that Fe, Al, Mn, Cr, Cd, Pb, and As associated with tailings from the Fundão dam affected different freshwater compartments (water, sediments, and biota), causing damage to watercourses and biodiversity. Our results indicate contamination in the coastal environment and that the mangrove ecosystem acts as a sink.

Changes observed in the carbon assimilation (A) of both species reflect changes in the efficiency of photosynthetic machinery as a result of higher concentrations of leaf metals. Khan et al. [77] suggested that the inhibition of this process, stimulated by trace elements, may be due to lower ATP and NADPH utilization, non-photochemical suppression, and a reduced rate of electron transport in photosystem II (PSII), which, according to the authors, decreases the quantum yield of electron transport and net photosynthesis in plants. The results indicate that trace elements, although essential nutrients, can interfere with the physiological performance of the species.

Similarly, the presence of trace elements has been documented as a major cause of changes in the oxidative metabolism of cells [21]. The unifying factor in determining the toxicity of metals is the generation of reactive oxygen species (ROS), caused mainly by the imbalance between pro-oxidant and antioxidant homeostasis [78]. According to Gupta et al. [79], PSII is a possible target of inhibition by ROS. DPPH• data suggests that the highest Mn, Cu, and Zn values altered the oxidative metabolism of *R. mangle* and *L. racemosa*. These metals can be considered highly toxic, depending on the plant and the concentration of the metal in the leaf tissue. The highest DPPH• (IC50), observed for *R. mangle* in the presence of Mn and *L. racemosa* in the presence of Cu and Zn, occurred in the estuaries of São Mateus and Caravelas, inferring a lower antioxidant capacity for these species and was justified by the lower values of A, Chla, and Chlb. A possible reason for the symptoms of oxidative stress may be due to the reduced efficiency of antioxidant defense by Cu<sup>2+</sup> and Mn<sup>2+</sup> [80,81]. The alteration in the activity of key enzymes of the antioxidant system, caused by higher concentrations of Cu and Mn, induces the degradation of Chla, with an increase in pheophytin a, pheophytin b, and total concentrations in leaves (pheophytinization), indicating a stress condition for the plant [81,82]. Under excess Mn, chlorophyll content and photosynthesis are highly affected, with a decrease in CO<sub>2</sub> fixation and the efficiency of electron flow in the chloroplast, the main source of ROS. Under low carbon fixation, excited chlorophyll molecules can generate <sup>1</sup>O<sub>2</sub> (singlet oxygen) which is extremely deleterious for photosynthetic reactions [83,84]. In most cases, excess Zn also generates reactive oxygen species [85], changes in electron transport, and membrane permeability [86].

According to Wang et al. [87], the mechanisms directly related to the reduction of photopigments are the replacement of the central magnesium in the porphyrin ring of the chlorophyll molecule, mainly by Mn, Cu, and Zn. Consequently, the cells accumulate protoporphyrin, and pigment synthesis is blocked [88]. Cheng et al. [89] and Naidoo et al. [90] showed that trace metals can decrease the chlorophyll content in mangrove species. In contrast, MacFarlane et al. [91] reported that in native plants such as mangroves, the accumulation of metals in the leaf tissue may not affect the content of chlorophylls. However, in this study, chlorophyll concentrations were altered in *R. mangle* in São Mateus, but mainly in *L. racemosa* located in São Mateus and Caravelas; this is supported by lower magnesium values and by the Chla/Chlb ratio (Figure 4). Elefteriou and Karataglis [92] observed that lower concentrations of chlorophyll occurred in an excess of Cu, as well as ultrastructural changes in chloroplasts such as the reduction in thylakoid membranes. Decreases in chlorophyll values can compromise the energy capture efficiency of PSII and reduce electron transport [93]. Reductions in the content of Chla and the Chla/Chlb ratio can be observed before any visible symptom of toxicity, indicating that such parameters can be used as sensitive indicators of metal stress [87]. Chlorophyll-a is considered more susceptible to oxidation than Chlb. The greater reduction in Chla compared to Chlb (Figure 4A,B) in *L. racemosa* may be due to the increased conversion of Chla to Chlb or, conversely, the lower reversion of Chlb to Chla [94]. The regulation of this process can be altered by metal

stress [95]. Accordingly, the behavior of *L. racemosa* can be considered a response to toxicity due to Cu and Zn. It is worth mentioning that the significant negative correlation between Chla and Fe-f ( $r = -0.094$ ,  $p < 0.01$ ), Mn-f ( $r = -0.074$ ,  $p < 0.01$ ), Cu-f ( $r = -0.072$ ,  $p < 0.05$ ), and Pb-f ( $r = -0.094$ ,  $p < 0.05$ ) in *R. mangle* (Figures 4 and 5) suggests that these metals also interfered in the synthesis of pigment for this species.

The bioconcentration factor, calculated as the ratio between the total metal in the leaf tissue and the metal concentration in the sediment, can estimate the potential for the bioaccumulation of plant metals and the plant-sediment interaction [96]. BCFs showed different patterns between metals and species (Table 2). In general, these differences are related to metals, but the physicochemical characteristics of sediments can also have implications for determining whether metals accumulate in plant tissues [97]. The low Fe BCF common to both species possibly results from the low availability of the metal present in the form of oxides and the physiological parameters, mainly, the root system that acts as a barrier to Fe transfer [52]. However, such behavior did not prevent this metal from altering the synthesis of chlorophylls as mentioned above. The Mn showed relatively low concentrations in the leaf tissue of *L. racemosa*, which is probably also related to the lower concentrations of this metal in the sediments. However, the fact that Mn is easily translocated from the root to the leaves by the xylem makes it highly bioavailable, resulting in a higher BCF than other metals. For *R. mangle* this is even more visible, considering that the characteristic anoxic sediment of this species generally precipitates some metals such as sulfates. Bernini et al. [73] found similar results for *R. mangle* in the São Mateus River estuary. The low BCF of Zn did not prevent the toxic action of the metal on the leaf tissues of *L. racemosa*. Cu showed a similar behavior concerning toxicity, with a BCF greater than 1 for this species. Despite Cu and Zn being considered essential micronutrients for plants, a higher concentration of these metals altered some functions of the physiology of the species, mainly of *L. racemosa*, as already mentioned. According to Chettri et al. [94], Pb is bound almost exclusively to the cell wall and is unlikely to have a direct effect on plant metabolism. However, if the Pb concentration in the tissues reflects the level of environmental contamination [98], the results of this study show high contamination compared to the Pb concentration in leaves of *L. racemosa* and *R. mangle* in impacted areas in the states of Rio de Janeiro and Espírito Santo, respectively [40,41], which receives effluents from nearby chemical, metallurgical, and steelmaking industries. Finally, it is important to consider that Pb and Cu are toxic elements to fauna and the bioaccumulation of these elements in leaves may transfer them to the food web by biomagnification. Caravelas, São Mateus, and Piraquê-Mirim are important habitats for mangrove crabs that have commercial interest. These places have an important protected marine area in the South Atlantic involving coral reefs and mangroves, such as Abrolhos Park and Costa das Algas.

The results of this study corroborate the hypotheses of Analuddian et al. [56], i.e., that the phylogeny of each mangrove species and their physiological behavior is in response to growth in different situations of contamination by heavy metals. More than that, the diversity of mangroves could explain the environmental resistance to the increased pollution of the coastal environment. The results also indicate that the mangrove ecosystem in the area affected by the Fundão tailings is a sink for trace elements dumped in the coastal zone. The different species of mangrove flora are acting as a source of bioremediation, accumulating the trace elements and heavy metals in their tissues, indicated here by leaf concentration. However, contamination is persistent in the Doce basin and has a long-term impact on the mangrove ecosystem. The region has a low diversity of flora species and a decrease in physiological performance could lead to the collapse of the mangrove ecosystem under another environmental stressor, such as a decrease in rainfall.

## 5. Conclusions

*R. mangle* and *L. racemosa* showed different behaviors concerning the concentration of metals in the sediment and, consequently, the effects of absorption on their leaf tissues. Both species showed adjustments in their physiological responses such as an alteration in

chlorophyll synthesis and carbon assimilation, stimulated by the production of reactive oxygen species and verified by higher values of DPPH• and by the negative correlations between leaf metals, pigments, and carbon assimilation. High concentrations of leaf Pb and Cu may also be indicative of contamination in the mangrove ecosystem, especially in fauna due to the trophic web. Although the metal uptake by mangroves provides short-term bioremediation, the associated decrease in carbon assimilation and primary productivity may reduce or eliminate mangrove ecosystem services, including metal uptake, in the long term.

**Supplementary Materials:** The following supporting information can be downloaded at: <https://www.mdpi.com/article/10.3390/coasts3020008/s1>, Table S1. Measurements of salinity in the interstitial water of sediments with the presence of *Rhizophora mangle* and *Laguncularia racemosa* in the Piraquê-Mirim, São Mateus, and Caravelas estuaries.

**Author Contributions:** V.D. carried out the experiments, writing, revising, and editing the manuscript, the statistical and multivariate analyzes, and prepared the figures and tables; M.M.P.T. designed the project and proposed the methodology, participated in the discussion, review and editing of the manuscript, acquired funding, and project administration; A.A.F., A.R.F. and I.G. participated in the manuscript review. M.B.d.R. contributed to experiments and the revision of the manuscript. M.A.d.O. contributed to experiments. All authors have read and agreed to the published version of the manuscript.

**Funding:** This research was developed under the Aquatic Biodiversity Monitoring Program, Environmental Area I, established by the Technical-Scientific Cooperation Agreement n° 30/2018 between the Espírito Santo Foundation of Technology (FEST) and Renova Foundation, published in Brazil's Official Gazette (Diário Oficial da União).

**Institutional Review Board Statement:** Not applicable.

**Informed Consent Statement:** Not applicable.

**Data Availability Statement:** The dataset generated during and/or analyzed during the current study is available from the corresponding author upon reasonable request.

**Acknowledgments:** We thank the Graduate Program in Environmental Oceanography (PPGOAM), Mangrove Ecology Laboratory, Soil Laboratory, Plant Mineral Nutrition Laboratory, Plant Ecophysiology Laboratory, and Experimental Farm at the Federal University of Espírito Santo (UFES) and the Chemical and Pharmaceutical Analysis Laboratory at the Federal University of Santa Maria (UFSM) and the Research Groups on Mangrove Ecology and Ecophysiology of Mangroves for their support in the fieldwork. The authors also thank the journal's anonymous reviewers for their valuable contributions to the final version of the manuscript.

**Conflicts of Interest:** The authors declare no conflict of interest.

## References

1. Chai, M.; Shen, X.; Li, R.; Qiu, G. The risk assessment of heavy metals in Futian mangrove forest sediment in Shenzhen Bay (South China) based on SEM–AVS analysis. *Mar. Pollut. Bull.* **2015**, *97*, 431–439. [[CrossRef](#)] [[PubMed](#)]
2. Tam, N.F.Y.; Wong, Y.S. Spatial variation of heavy metals in surface sediments of Hong Kong mangrove swamps. *Environ. Pollut.* **2000**, *110*, 195–205. [[CrossRef](#)] [[PubMed](#)]
3. Bouillon, S.; Borges, A.V.; Castañeda-Moya, E.; Diele, K.; Dittmar, T.; Duke, N.C.; Twilley, R.R. Mangrove production and carbon sinks: A revision of global budget estimates. *Glob. Biogeochem. Cycles* **2008**, *22*, 1–12. [[CrossRef](#)]
4. Sasmito, S.D.; Sillanpaa, M.; Hayes, M.A.; Bachri, S.; Saragi-Sasmito, M.F.; Sidik, F.; Hanggara, B.B.; Mofu, W.Y.; Rumbiak, V.I.; Hendri, T.S.; et al. Mangrove blue carbon stocks and dynamics are controlled by hydrogeomorphic settings and land-use change. *Glob. Chang. Biol.* **2020**, *26*, 3028–3039. [[CrossRef](#)] [[PubMed](#)]
5. CONAMA (Conselho Nacional de Meio Ambiente). Resolução Conama N. 457 de 01 de Novembro de 2012. 2012. Available online: <http://www.mma.gov.br> (accessed on 10 January 2019).
6. Marta-Almeida, M.; Mendes, R.; Amorim, F.N.; Cirano, M.; Dias, J.M. Fundação Dam collapse: Oceanic dispersion of River Doce after the greatest Brazilian environmental accident. *Mar. Pollut. Bull.* **2016**, *112*, 359–364. [[CrossRef](#)] [[PubMed](#)]
7. Segura, F.R.; Nunes, E.A.; Paniz, F.P.; Paulelli, A.C.C.; Rodrigues, G.B.; Braga, W.; Filho, W.R.P.; Barbosa Júnior, F.; Cerchiaro, G.; Silva, F.F.; et al. Potential risks of the residue from Samarco's mine dam burst (Bento Rodrigues, Brazil). *Environ. Pollut.* **2016**, *218*, 813–825. [[CrossRef](#)]

8. Bianchini, A.; Da Silva, C.C.; Lauer, M.M.; Jorge, M.B.; Costa, P.G.; Marques, J.A.; Marangoni, L.F.B.; Jesulich, A.C.; Taylor, A.J.; Luz, D.C.; et al. *Avaliação do Impacto da Lama/Pluma Samarco Sobre os Ambientes Costeiros e Marinheiros (ES e BA) Com ênfase Nas Unidades de Conservação. 1a Expedição do Navio de Pesquisa Soloncy Moura do CEPISUL/ICMBio*; Ministério do Meio Ambiente. Instituto Chico Mendes de Conservação da Biodiversidade—ICMBio; Diretoria de Pesquisa, Avaliação e Monitoramento da Biodiversidade: Brasília, DF, Brazil, 2016; 62p.
9. Queiroz, H.M.; Nóbrega, G.N.; Ferreira, T.O.; Almeida, L.S.; Romero, T.B.; Santaella, S.T.; Bernardino, A.F.; Otero, X.L. The Samarco mine tailing disaster: A possible time-bomb for heavy metals contamination? *Sci. Total Environ.* **2018**, *637*, 498–506. [[CrossRef](#)]
10. Tognella, M.M.P.; Falqueto, A.R.; Espinoza, H.D.C.F.; Gontijo, I.; Gontijo, A.B.P.L.; Fernandes, A.A.; Schmidt, E.R.; Soares, M.L.G.; Chaves, F.O.; Schmidt, A.J.; et al. Mangroves as traps for environmental damage to metals: The case study of the Fundão Dam. *Sci. Total Environ.* **2022**, *806*, 150452. [[CrossRef](#)]
11. Conrad, S.R.; Santos, I.R.; Brown, D.R.; Sanders, L.M.; van Santen, M.L.; Sanders, C.J. Mangrove sediments reveal records of development during the previous century (Coffs Creek estuary, Australia). *Mar. Pollut. Bull.* **2017**, *122*, 441–445. [[CrossRef](#)]
12. Machado, A.A.S.; Wood, C.M.; Bianchini, A.; Gillis, P.A. Responses of biomarkers in wild freshwater mussels chronically exposed to complex contaminant mixtures. *Ecotoxicology* **2014**, *23*, 1345–1358. [[CrossRef](#)]
13. Zhou, Q.; Zhang, J.; Fu, J.; Shi, J.; Jiang, G. Biomonitoring: An appealing tool for assessment of metal pollution in the aquatic ecosystem. *Anal. Chim. Acta* **2008**, *606*, 135–150. [[CrossRef](#)] [[PubMed](#)]
14. Lasat, M.M. Phytoextraction of toxic metals. *J. Environ. Qual.* **2002**, *31*, 109–120. [[CrossRef](#)] [[PubMed](#)]
15. Verbruggen, N.; Hermans, C.; Schat, H. Molecular mechanisms of metal hyperaccumulation in plants. *New Phytol.* **2009**, *181*, 759–776. [[CrossRef](#)] [[PubMed](#)]
16. Onofre, D.E.; Regina, C.; José, J.; Nano, W.; Maria, R.; Queiroz, D.S. Biodisponibilidade de metais traços nos sedimentos de manguezais da porção norte da Baía de Todos os Santos, Bahia, Brasil. *Rev. Biol. E Ciências Terra* **2007**, *7*, 65–82. Available online: <https://www.redalyc.org/articulo.oa?id=50007208> (accessed on 13 September 2020).
17. Mehana, E.S.E.; Khafaga, A.F.; Elbehi, S.S.; El-Hack, M.E.A.; Naiel, M.A.E.; Bin-Jumah, M.; Othaman, S.I.; Allam, A.A. Biomonitoring of heavy metal pollution using acanthocephalans parasite in ecosystem: An updated overview. *Animals* **2020**, *10*, 811. [[CrossRef](#)]
18. MacFarlane, G.R.; Koller, C.E.; Blomberg, S.P. Accumulation and partitioning of heavy metals in mangroves: A synthesis of field-based studies. *Chemosphere* **2007**, *69*, 1454–1464. [[CrossRef](#)]
19. Yan, Z.; Sun, X.; Xu, Y.; Zhang, Q.; Li, X. Accumulation and Tolerance of Mangroves to Heavy Metals: A Review. *Curr. Pollut. Rep.* **2017**, *3*, 302–317. [[CrossRef](#)]
20. Agoramoorthy, G.; Chenfa, H.M.J. Threat of heavy metal pollution in halophytic and mangrove plants of Tamil Nadu, India. *Environ. Pollut.* **2008**, *155*, 320–326. [[CrossRef](#)]
21. Vangronsveld, J.; Clijsters, H. Toxic effects of metals. In *Plants and the Chemical Elements: Biochemistry, Uptake, Tolerance and Toxicity*; Farago, M.E., Ed.; VCH Press: Weinheim, Germany, 1994; pp. 149–177. [[CrossRef](#)]
22. Bhaduri, A.; Fulekar, M.H. Antioxidant enzyme response of plants to heavy metal stress. *Rev. Environ. Sci. Biotechnol.* **2012**, *11*, 55–69. [[CrossRef](#)]
23. Balk, J.; Pilon, M. Ancient and essential: The assembly of iron–sulfur clusters in plants. *Trends Plant Sci.* **2011**, *16*, 218–226. [[CrossRef](#)]
24. Ure, A.M.; Davidson, C.M. *Chemical Speciation in the Environment*; Blackwell Science: Glasgow, UK, 2001. [[CrossRef](#)]
25. Du Laing, G.; Bogaert, N.; Tack, F.M.G.; Verloo, M.G.; Hendrickx, F. Heavy metal contents (Cd, Cu, Zn) in spiders (*Pirata piraticus*) living in intertidal sediments of the river Scheldt estuary (Belgium) as affected by substrate characteristics. *Sci. Total Environ.* **2002**, *289*, 71–81. [[CrossRef](#)] [[PubMed](#)]
26. Marchand, C.; Lallier-Vergès, E.; Baltzer, F.; Albéric, P.; Cossa, D.; Baillif, P. Heavy metals distribution in mangrove sediments along the mobile coastline of French Guiana. *Mar. Chem.* **2006**, *98*, 1–17. [[CrossRef](#)]
27. Ahmed, K.; Mehedi, Y.; Haque, R.; Mondol, P. Heavy metal concentrations in some macrobenthic fauna of the Sundarbans mangrove forest, southwest coast of Bangladesh. *Environ. Monit. Assess.* **2011**, *177*, 505–514. [[CrossRef](#)] [[PubMed](#)]
28. Ibama. Laudo Técnico Preliminar: Impactos Ambientais Decorrentes do Desastre Envolvendo o Rompimento da Barragem de Fundão, em Mariana, Minas Gerais. Instituto Brasileiro do Meio Ambiente e dos Recursos Naturais Renováveis. 2015. Available online: [http://www.ibama.gov.br/phocadownload/barragemdefundao/laudos/laudo\\_tecnico\\_preliminar\\_ibama.pdf](http://www.ibama.gov.br/phocadownload/barragemdefundao/laudos/laudo_tecnico_preliminar_ibama.pdf) (accessed on 13 February 2019).
29. Hadlich, H.L.; Venturini, N.; Martins, C.C.; Hatje, V.; Tinelli, P.; Gomes, L.E.O.; Bernardino, A.F. Multiple biogeochemical indicators of environmental quality in tropical estuaries reveal contrasting conservation opportunities. *Ecol. Indic.* **2018**, *95*, 21–31. [[CrossRef](#)]
30. Tognella, M.M.P.; Leopoldo, R.V.S.; Oliveira, C.P.; Pascoalini, S.S.; Silva, E.D. Diversidade estrutural das florestas de mangue da costa central e norte do Espírito Santo: Contribuições para entendimento de funções ecossistêmicas. *Enciclopédia Biosf.* **2020**, *17*, 178–193. [[CrossRef](#)]

31. Dias, J.A. *Análise Sedimentar e o Conhecimento dos Sistemas Marinhos—Uma Introdução à Oceanografia Geológica*; Faro, Universidade do Algarve: Algarve, Portugal, 2004. Available online: [https://www.researchgate.net/publication/236551412\\_A\\_ANALISE\\_SEDIMENTAR\\_E\\_O\\_CONHECIMENTOS\\_DOS\\_SISTEMAS\\_MARINHOS\\_Uma\\_Introducao\\_a\\_Oceanografia\\_Geologica](https://www.researchgate.net/publication/236551412_A_ANALISE_SEDIMENTAR_E_O_CONHECIMENTOS_DOS_SISTEMAS_MARINHOS_Uma_Introducao_a_Oceanografia_Geologica) (accessed on 25 March 2019).
32. Wentworth, C.K. A scale of grade and class terms for clastic sediments. *J. Geol.* **1922**, *30*, 377–392. Available online: <http://www.jstor.org/stable/30063207> (accessed on 13 January 2019). [[CrossRef](#)]
33. Suguio, K. *Geologia Sedimentar*; Blucher: São Paulo, Brazil, 2003; ISBN 9788521203179.
34. Santos, H.G.; Jacomine, P.K.T.; Anjos, L.H.C.; Oliveira, V.Á.; Lumbresas, J.F.; Coelho, M.R.; Almeida, J.A.; Filho, J.A.; Oliveira, J.B.; Cunha, T.J.F. *Sistema Brasileiro de Classificação de Solos*; Embrapa Solos: Brasília, Brazil, 2018; ISBN 9788570358004.
35. United States Environmental Protection Agency (USEPA) Electronic Code of Federal Regulations, Title 40—Protection of Environment, Part 423—Steam Electric Power Generating Point Source Category, Appendix A to Part 423–126, Priority Pollutants. 2013. Available online: <https://www.ecfr.gov/cgi-bin/text-idx?node=pt40.31.423&rgn=div5> (accessed on 16 July 2020).
36. Buchman, M.F. NOAA Screening Quick Reference Tables, NOAA OR&R Report 08-1, Seattle WA, Office of Response and Restoration Division, National Oceanic and Atmospheric Administration. 2008. Available online: <https://repository.library.noaa.gov/view/noaa/9327> (accessed on 10 January 2019).
37. Blanchar, R.W.; Rehm, G.; Caldwell, A.C. Sulfur in plant material digestion with nitric and perchloric acids. *Soil Sci. Soc. Am. Proc.* **1965**, *29*, 71–72. [[CrossRef](#)]
38. Malavolta, E.; Vittì, C.C.; Oliveira, S.A. *Avaliação do Estado Nutricional das Plantas: Princípios e Aplicações*; Esalq-USP: Piracicaba, Brazil, 1997.
39. Cuzzuol, G.R.F.; Campos, A. Aspectos nutricionais na vegetação de manguezal do estuário do rio Mucuri, Bahia, Brasil. *Rev. Bras. Bot.* **2001**, *24*, 227–234. [[CrossRef](#)]
40. Machado, W.; Silva-Filho, E.V.; Oliveira, R.R.; Lacerda, L.D. Trace metal retention in mangrove ecosystems in Guanabara Bay, SE Brazil. *Mar. Pollut. Bull.* **2002**, *44*, 1277–1280. [[CrossRef](#)]
41. Souza, I.C.; Morozesk, M.; Duarte, I.D.; Bonomo, M.M.; Rocha, L.D.; Furlan, L.M.; Arrivabene, H.P.; Monferran, M.V.; Matsumoto, S.T.; Milanez, C.R.D.; et al. Matching pollution with adaptive changes in mangrove plants by multivariate statistics. A case study, *Rhizophora mangle* from four neotropical mangroves in Brazil. *Chemosphere* **2014**, *108*, 115–124. [[CrossRef](#)]
42. Dal Prá, V.; Dolwitsch, C.B.; Da Silveira, G.D.; Porte, L.; Frizzo, C.; Tres, M.V.; Da Rosa, M.B. Supercritical CO<sub>2</sub> extraction, chemical characterization and antioxidant potential of *Brassica oleracea* var capitata against HO<sup>•</sup>, O<sup>•−2</sup> and ROO<sup>•</sup>. *Food Chem.* **2013**, *141*, 3954–3959. [[CrossRef](#)] [[PubMed](#)]
43. Arar, E.J. Determination of Chlorophylls a and b and Identification of Other Pigments of Interest in Marine and Freshwater Algae Using High-Performance Liquid Chromatography with Visible Wavelength Detection. EPA Method 447.0 447, 1–20. 1997. Available online: [https://cfpub.epa.gov/si/si\\_public\\_record\\_report.cfm?Lab=NERL&dirEntryId=309414](https://cfpub.epa.gov/si/si_public_record_report.cfm?Lab=NERL&dirEntryId=309414) (accessed on 18 December 2018).
44. Cruz, C.D. Programa Genes—Ampliado e integrado aos aplicativos R, Matlab e Selegen. *Acta Sci. Agron.* **2016**, *38*, 547–552. [[CrossRef](#)]
45. R Core Team. *The R Project for Statistical Computing*; R Foundation for Statistical Computing: Vienna, Austria, 2021. Available online: <https://www.R-project.org/> (accessed on 25 November 2021).
46. Wickham, H. *ggplot2: Elegant Graphics for Data Analysis*; Springer: New York, NY, USA, 2016.
47. Le, S.; Josse, J.; Husson, F. FactoMineR: An R package for multivariate analysis. *J. Stat. Softw.* **2008**, *25*, 1–18. [[CrossRef](#)]
48. Kassambara, A.; Mundt, F. Factoextra: Extract and Visualize the Results of Multivariate Data Analyses, R Package Version 1.0.5; 2017. Available online: <https://CRAN.Rproject.org/package=factoextra> (accessed on 25 November 2021).
49. Thuleau, S.; Husson, F. FactoInvestigate: Automatic Description of Factorial Analysis, R Package Version 1.7. 2020. Available online: <https://CRAN.R-project.org/package=FactoInvestigate> (accessed on 25 November 2021).
50. Bartoli, G.; Papa, S.; Sagnella, E.; Fioretto, A. Heavy metal content in sediments along the Calore River: Relationships with physical e chemical characteristics. *J. Environ. Manag.* **2012**, *95*, S9–S14. [[CrossRef](#)] [[PubMed](#)]
51. Miola, B.; Morais, J.O.D.; Pinheiro, L.S. Trace metal concentrations in tropical mangrove sediments, NE Brazil. *Mar. Pollut. Bull.* **2016**, *102*, 206–209. [[CrossRef](#)]
52. Marchand, C.; Fernandez, J.M.; Moreton, B. Trace metal geochemistry in mangrove sediments and their transfer to mangrove plants (New Caledonia). *Sci. Total Environ.* **2016**, *562*, 216–227. [[CrossRef](#)] [[PubMed](#)]
53. Liu, W.J.; Zhu, Y.G.; Hu, Y.; Williams, P.H.; Gault, A.G.; Meharg, A.A.; Charnock, J.M.; Smith, F.A. Arsenic sequestration in iron plaque, its accumulation and speciation in mature rice plants (*Oryza sativa* L.). *Environ. Sci. Technol.* **2006**, *40*, 5730–5736. [[CrossRef](#)]
54. Tam, N.F.Y.; Wong, Y.S. Mangrove soils in removing pollutants from municipal wastewater of different salinities. *J. Environ. Qual.* **1999**, *28*, 556–564. [[CrossRef](#)]
55. Ye, H.; Zang, S.; Xiao, H.; Zhang, L. Speciation and ecological risk of heavy metals and metalloid in the sediments of Zhalong Wetland in China. *Int. J. Environ. Sci. Technol.* **2015**, *12*, 115–124. [[CrossRef](#)]
56. Analuddin, K.; Sharma, S.; Jamili, Septiana, A.; Sahidind, I.; Riansee, U.; Nadaoka, K. Heavy metal bioaccumulation in mangrove ecosystem at the coral triangle ecoregion, Southeast Sulawesi, Indonesia. *Mar. Pollut. Bull.* **2017**, *125*, 472–480. [[CrossRef](#)]
57. Kabata-Pendias, A. *Trace Elements in Soils and Plants*; CRC Press: Boca Raton, FA, USA, 2010. [[CrossRef](#)]

58. Araújo Júnior, C.J.M.; Ferreira, T.O.; Suarez-Abelenda, M.; Nóbrega, G.N.; Albuquerque, A.G.B.M.; de Ca Bezerra, A.; Otero, X.L. The role of bioturbation by *Ucides cordatus* crab in the fractionation and bioavailability of trace metals in tropical semiarid mangroves. *Mar. Pollut. Bull.* **2016**, *111*, 194–202. [CrossRef] [PubMed]
59. Lovley, D.R.; Holmes, D.E.; Nevin, K.P. Dissimilatory Fe(III) and Mn(IV) reduction. *Adv. Microb. Physiol.* **2004**, *49*, 219–286. [CrossRef] [PubMed]
60. RRDM. *Relatório Anual 2019 do PMBA/Fest-RRDM—Anexo 5-Manguezal-RT-21 RRDM/NOV 19*; Fundação Espírito-Santense de Tecnologia (Fest)/Rede Rio Doce Mar (RRDM): Vitória, ES, Brazil, 2019; 600p.
61. RRDM. *Relatório Anual 2020 do PMBA/Fest-RRDM-Evolução Espaço-Temporal na Qualidade Ambiental e na Biodiversidade no Ambiente Costeiro-RT-36C RRDM/DEZ 20*; Fundação Espírito-Santense de Tecnologia (Fest)/Rede Rio Doce Mar (RRDM): Vitória, ES, Brazil, 2020; 422p.
62. Chakraborty, P.; Ramteke, D.; Chakraborty, S. Geochemical partitioning of Cu and Ni in mangrove sediments: Relationships with their bioavailability. *Mar. Pollut. Bull.* **2015**, *93*, 194–201. [CrossRef]
63. Chakraborty, P.; Chakraborty, S.; Ramteke, D.; Chennuri, K. Kinetic speciation and bioavailability of copper and nickel in mangrove sediments. *Mar. Pollut. Bull.* **2014**, *88*, 224–230. [CrossRef] [PubMed]
64. Santos, L.M.M.; Souza, R.C.; Anunciação, D.S.; Moreira, I.T.A.; Santos, V.L.C.S.; Viana, Z.C.V. Evaluation of chemical elements content in mangroves island of Itaparica, Bahia, Brazil. *Acta Bras.* **2018**, *2*, 15–20. [CrossRef]
65. Sipos, P.; Nemeth, T.; Mohai, I. Distribution and possible immobilization of lead in a forest soil (Luvisol) profile. *Environ. Geochem. Health* **2005**, *27*, 1–10. [CrossRef]
66. Bromenschenkel, V.C.S.; Tognella, M.M.P. Population estimate and extractive potential of uçá crab in the post-closed season: Subsidies for management in a Conservation Unit of sustainable use. *Res. Soc. Dev.* **2020**, *9*, e25791210992. [CrossRef]
67. ICMBio. Plano de Manejo da Reserva Extrativista de Cassurubá—Diagnóstico—Volume I. Instituto Chico Mendes de Conservação da Biodiversidade. 2018. Available online: [https://www.gov.br/icmbio/pt-br/assuntos/biodiversidade/unidade-de-conservacao/unidades-de-biomas/marinho/lista-de-ucs/resex-de-cassuruba/arquivos/plano\\_de\\_manejo\\_resex\\_de\\_cassuruba\\_diagnostico\\_vol1.pdf](https://www.gov.br/icmbio/pt-br/assuntos/biodiversidade/unidade-de-conservacao/unidades-de-biomas/marinho/lista-de-ucs/resex-de-cassuruba/arquivos/plano_de_manejo_resex_de_cassuruba_diagnostico_vol1.pdf) (accessed on 19 April 2022).
68. Lutts, S.; Lefèvre, I. How can we take advantage of halophyte properties to cope with heavy metal toxicity in salt-affected areas? *Ann. Bot.* **2015**, *115*, 1–20. [CrossRef]
69. Machado, W.; Gueiros, B.B.; Lisboa-Filho, S.D.; Lacerda, L.D. Trace metals in mangrove seedlings: Role of iron plaque formation. *Wetl. Ecol. Manag.* **2005**, *13*, 199–206. [CrossRef]
70. Lacerda, L.D.; Rezende, C.E.; José, D.V.; Francisco, M.C. Metallic composition of leaves from the Southeastern Brazilian coast. *Rev. Bras. Biol.* **1986**, *46*, 395–399.
71. Medina, E.; Giarizzo, T.; Menezes, M.; Carvalholira, M.; Carvalho, E.A.; Peres, A.; Silva, B.; Vilhena, R.; Reise, A.; Braga, F.C. Mangal communities of the Salgado Paraense: Ecological heterogeneity along the Bragança peninsula assessed through soil and leaf analysis. *Amazoniana* **2001**, *16*, 397–416. Available online: <http://hdl.handle.net/21.11116/0000-0004-9629-5> (accessed on 11 April 2023).
72. Arrivabene, H.P.; Souza, I.C.; Có, W.L.O.; Conti, M.M.; Wunderlin, D.A.; Milanez, C.R.D. Effect of pollution by particulate iron on the morphoanatomy, histochemistry, and bioaccumulation of three mangrove plant species in Brazil. *Chemosphere* **2015**, *127*, 27–34. [CrossRef] [PubMed]
73. Bernini, E.; Silva, M.A.B.; Carmo, T.M.; Cuzzuol, G.R.F. Composição química do sedimento e de folhas das espécies do manguezal do estuário do Rio São Mateus, Espírito Santo, Brasil. *Rev. Bras. Bot.* **2006**, *29*, 689–699. [CrossRef]
74. Lacerda, L.D.; Martinelli, L.A.; Rezende, C.E.; Mozeto, A.A.; Ovalle, A.R.C.; Victoria, R.L.; Silva, C.A.R.; Nogueira, F.B. The fate of trace metals in suspended matter in a mangrove creek during a tidal cycle. *Sci. Total Environ.* **1988**, *75*, 169–180. [CrossRef]
75. Lacerda, L.D.; Rezende, C.E.; José, D.V.; Wasserman, J.C.; Francisco, M.C. Mineral concentrations in leaves of mangrove trees. *Biotropica* **1985**, *17*, 21–27. [CrossRef]
76. Dechen, A.R.; Nachtigall, G. Micronutrientes. In *Nutrição Mineral de Plantas*; Fernandes, M.S., Ed.; SBCS: Viçosa, Brazil, 2006; pp. 327–354, ISBN 8586504025.
77. Khan, M.; Neeha, N.; Ifthekhar, A.; Muhammad, A.; Muhammad, R.; Parvaiz, A.; Shafaqat, A. Regulation of Photosynthesis Under Metal Stress. In *Photosynthesis, Productivity and Environmental Stress*; Ahmad, P., Ahanger, M.A., Alyemeni, M.N., Alam, P., Eds.; John Wiley & Sons Ltd.: Hoboken, NJ, USA, 2020; pp. 95–105.
78. Ghori, N.H.; Ghori, T.; Hayat, M.Q.; Imadi, S.R.; Gul, A.; Altay, V.; Ozturk, M. Heavy metal stress and responses in plants. *Int. J. Environ. Sci. Technol.* **2019**, *16*, 1807–1828. [CrossRef]
79. Gupta, M.; Cuypers, A.; Vangronsveld, J.; Clijsters, H. Copper affects the enzymes of the ascorbate-glutathione cycle and its related metabolites in the roots of *Phaseolus vulgaris*. *Physiol. Plant.* **1999**, *106*, 262–267. [CrossRef]
80. Pätsikkä, E.; Kairavuo, M.; Sersen, F.; Aro, E.M.; Tyystjärvi, E. Excess copper predisposes photosystem II to photoinhibition in vivo by outcompeting iron and causing decrease in leaf chlorophyll. *Plant Physiol.* **2002**, *129*, 1359–1367. [CrossRef]
81. Millaleo, R.; Reyes-Díaz, M.; Ivanov, A.G.; Mora, M.L.; Alberdi, M. Manganese as essential and toxic element for plants: Transport, accumulation and resistance mechanisms. *J. Soil Sci. Plant Nutr.* **2010**, *10*, 476–494. [CrossRef]
82. Gururani, M.A.; Venkatesh, J.; Tran, L.S.P. Regulation of photosynthesis during abiotic stress-induced photoinhibition. *Mol. Plant* **2015**, *8*, 1304–1320. [CrossRef]

83. Fernando, D.R.; Marshall, A.L.T.; Forster, P.I.; Hoebee, S.E.; Siegele, R.A. Multiple metal accumulation within, a manganese-specific genus. *Am. J. Bot.* **2013**, *100*, 690–700. [[CrossRef](#)] [[PubMed](#)]
84. Anjum, N.A.; Singh, H.P.; Khan, M.I.R.; Masood, A.; Per, T.S.; Negi, A.; Batish, D.R.; Khan, N.A.; Duarte, A.C.; Pereira, E.; et al. Too much is bad—An appraisal of phytotoxicity of elevated plant-beneficial heavy metal ions. *Environ. Sci. Pollut. Res.* **2015**, *22*, 3361–3382. [[CrossRef](#)]
85. Marschner, P. *Marschner's Mineral Nutrition of Higher Plants*; Academic Press: Cambridge, MA, USA, 2012. [[CrossRef](#)]
86. Wang, C.; Wang, X.; Wang, B.; Zhang, C.; Shi, X.; Zhu, C. Level and fate of heavy metals in the Changjiang estuary and its adjacent waters. *Oceanology* **2009**, *49*, 64–72. [[CrossRef](#)]
87. Wang, Y.; Zhou, L.; Zheng, X.; Qian, P.; Wu, Y. Influence of *Spartina alterniflora* on the mobility of heavy metals in saltmarsh sediments of the Yangtze River estuary, China. *Environ. Sci. Pollut. Res.* **2013**, *20*, 1675–1685. [[CrossRef](#)]
88. Küpper, H.; Šetlík, I.; Spiller, M.; Küpper, F.C.; Prášil, O. Heavy metal-induced inhibition of photosynthesis: Targets of in vivo heavy metal chlorophyll formation. *J. Phycol.* **2002**, *38*, 429–441. [[CrossRef](#)]
89. Cheng, H.; Tam, N.F.Y.; Wang, Y.S.; Li, S.Y.; Chen, G.Z.; Ye, Z.H. Effect of copper on growth, radial oxygen loss and root permeability of seedlings of mangroves *Bruguiera gymnorrhiza* and *Rhizophora stylosa*. *Plant Soil* **2012**, *359*, 255–266. [[CrossRef](#)]
90. Naidoo, G.; Hiralal, T.; Naidoo, Y. Ecophysiological response of the mangrove *Avicennia marina* to trace metal contamination. *Flora* **2014**, *209*, 63–72. [[CrossRef](#)]
91. MacFarlane, G.R.; Pulkownik, A.; Burchett, M.D. Accumulation and distribution of heavy metals in the grey mangrove *Avicennia marina* (Forsk.) Vierh.: Biological indication potential. *Environ. Pollut.* **2003**, *123*, 139–151. [[CrossRef](#)]
92. Elefteriou, E.P.; Karataglis, S. Ultrastructural and morphological characteristics of cultivated wheat growing on copper-polluted fields. *Bot. Acta* **1989**, *102*, 134–140. [[CrossRef](#)]
93. Kocheva, K.; Lambrev, P.; Georgiev, G.; Goltsev, V.; Karabaliiev, M. Evaluation of chlorophyll fluorescence and membrane injury in the leaves of barley cultivars under osmotic stress. *Bioelectrochemistry* **2004**, *63*, 121–124. [[CrossRef](#)]
94. Chettri, M.K.; Cook, C.M.; Vardaka, E.; Sawidis, T.; Lanaras, T. The effect of Cu, Zn and Pb on the chlorophyll content of the lichens *Cladonia convoluta* and *Cladonia rangiformis*. *Environ. Exp. Bot.* **1998**, *39*, 1–10. [[CrossRef](#)]
95. Ebbs, S.; Uchil, S. Cadmium and zinc induced chlorosis in Indian mustard [*Brassica juncea* (L.) Czern] involves preferential loss of chlorophyll b. *Photosynthetica* **2008**, *46*, 49–55. [[CrossRef](#)]
96. Bakshi, M.; Ghosh, S.; Chakraborty, D.; Hazra, S.; Chaudhuri, P. Assessment of potentially toxic metal (PTM) pollution in mangrove habitats using biochemical markers: A case study on *Avicennia officinalis* L. in and around Sundarban, India. *Mar. Pollut. Bull.* **2018**, *133*, 157–172. [[CrossRef](#)] [[PubMed](#)]
97. Petranich, E.; Acquavita, A.; Covelli, S.; Emili, A. Potential bioaccumulation of trace metals in halophytes from salt marshes of a northern Adriatic coastal lagoon. *J. Soils Sediments* **2017**, *17*, 1986–1998. [[CrossRef](#)]
98. Ong Che, R.G. Concentration of 7 heavy metals in sediments and mangrove root samples from Mai Po, Hong Kong. *Mar. Pollut. Bull.* **1999**, *39*, 269–279. [[CrossRef](#)]

**Disclaimer/Publisher's Note:** The statements, opinions and data contained in all publications are solely those of the individual author(s) and contributor(s) and not of MDPI and/or the editor(s). MDPI and/or the editor(s) disclaim responsibility for any injury to people or property resulting from any ideas, methods, instructions or products referred to in the content.